Interatomic forces breaking carbon-carbon bonds

Mat Tolladay,[*,†,¶] Fabrizio Scarpa,[†] and Neil L. Allan[‡]

†*Bristol Composites Institute, CAME School of Engineering, University of Bristol, Bristol, UK*

‡*School of Chemistry, University of Bristol, Bristol, UK*

¶*Current address: Department of Chemical Engineering, University of Bath, Bath, UK*

E-mail: m.j.tolladay@bath.ac.uk

Abstract

We compare computational methods for determining the force between carbon atoms in small organic molecules as a function of bond length, using density-functional theory, post-Hartree-Fock methods, density-functional tight-binding and two commonly used molecular mechanics potentials. Every method produces different quantitative results for the peak restorative force between the carbon atoms. Nevertheless, the electronic structure results predict very similar bond lengths at which this peak force occurs while the molecular mechanics potentials struggle to reproduce the behaviour of the electronic structure methods both qualitatively and quantitatively. Tight-binding results are broadly similar to those from the first-principles methods but depend markedly on which parameter sets are chosen. Methods that recover dynamic correlation predict higher peak forces than those that recover static correlation. This shows the importance of the electronic behaviour for the carbon-carbon interatomic forces relevant to the determination of the mechanical strength of materials at atomic-length scales.

Keywords

Carbon, mechanical properties, bonding

Introduction

Nanostructures are an increasingly important topic in material science, with potential uses in electronics,[1] hydrogen storage,[2] water purification,[3] catalysis[4] and composite materials.[5] Experimental investigation of nanostructures remains difficult and costly to perform and results often require verification through theoretical calculations. Simulating these structures requires modelling from a few hundred up to a few thousand atoms which is problematic for most electronic structure methods. The computational cost of these methods scales poorly with the number of electrons leading to limits on the size of the nanostructures which can be investigated.

There is a great deal of interest in using carbon nanostructures as components of composite materials. In order to understand which nanostructures are best suited to this task requires knowledge of what loads they can withstand and the degree of deformation to which they can be subjected. Determining mechanical properties, such as the tensile strength, of nanoscale devices experimentally is an exceptionally complex task due to the difficulty of manipulating them accurately and without causing damage while setting up the experiment. The alternative is to use simulations. Such calculations require accurate mathematical descriptions of bonds being stretched to breaking point and beyond. A few classical potentials claim to have the ability to achieve this and are regularly employed for simulating carbon based structures undergoing catastrophic failure. The two most common are Tersoff-Brenner type potentials[6,7] and the ReaxFF potential,[8] both used for predicting the strength of graphene nanoribbons[9–11] and fracture growth in graphene.[12–14] They rely on approximating the interatomic forces rather than explicitly determining them through electronic structure calculations. Computational chemistry has many tools capable of determining the electronic

structure but there is always a trade off between accuracy and computational expense and bond dissociation is known to be particularly challenging. It is important that reliable methods for simulating failure of nanostructures, containing thousands of atoms, are identified.

Intramolecular forces in molecular simulations are often calculated close to energy minima where the forces can be approximated as linear. Such forces are used primarily in chemical applications to calculate vibrational frequencies, to locate key points on potential energy surfaces and in molecular dynamics simulations. Another particularly important but much less common study is the investigation of atomic scale failure mechanisms of materials under mechanical stress, where bond lengths and angles are far from their equilibrium values. Failure at the *macroscale* is defined by the strength of a material: the peak stress the material can carry before catastrophic failure. Stress has units of force per unit area and the peak stress occurs at the peak force for a constant cross sectional area. From this perspective, a bond's tensile strength can be considered as the maximum force that it can withstand.[15] If a constant tensile force greater than this limit is applied to a pair of bonded atoms then it will overcome the restorative force of the bond, causing the atoms to dissociate. The peak restorative force occurs at the inflection point in the variation of the bond energy with bond length,[16] as shown in figure 1.

Determining values for this quantity experimentally is challenging but has been achieved using polysaccharide molecules covalently bonded to a substrate, using an atomic force microscope tip to apply a tensile force to the molecules.[15] One of the difficulties of such experiments is determining which bond breaks. This is possible *a posteriori* by comparison with theoretical calculations considering the various bonds in the test molecule and for those that attach it to the substrate.

Accurate electronic structure methods are computationally expensive. Methods such as density functional theory (DFT), Møller-Plesset perturbation theory and many others are capable of considerable accuracy but their costs scale poorly with system size. Furthermore, it is necessary to employ multi-reference methods to capture the energetics of bond breaking[17–20]

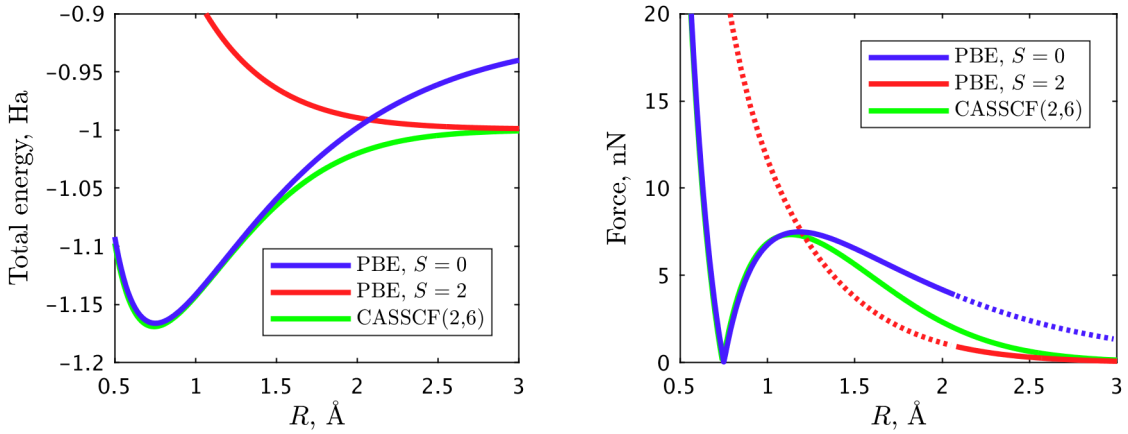

Figure 1: (a) total energy (hartree) of H_2 as a function of internuclear separation R (Å) and (b) magnitude of the force on a hydrogen atom in H_2 as a function of internuclear separation. Dotted lines indicate that the plotted state is not the single determinant ground state. The two PBE functional based density functional theory results are for where the electrons are spin paired ($S = 0$) and unpaired ($S = 2$), respectively. The spin-paired PBE calculation tends towards an incorrect energy as $R \to \infty$, higher than one hartree, and tends to this value more slowly than the CASSCF result. The $S = 2$ plot crosses the $S = 0$ curve at which point it becomes the single determinant ground state which leads to an unphysical discontinuity in the force at the crossing point. The complete active space self consistent field (CASSCF) result shows the correct physical behaviour as $R \to \infty$, approaching an energy value of one hartree, the energy of two hydrogen atoms at infinite separation. The multi reference CASSCF calculation contains contributions from a number of excited-state determinants so avoids the discontinuity seen in the DFT results.

due to the lack of size consistency and inability of single-reference methods to account for static correlation effects. This can be seen graphically in figure 1 which shows the potential energy and corresponding force for the H_2 molecule over a range of bond lengths. This figure shows the results of a single reference method, PBE based DFT, using two different spin states compared with the multi-reference method CASSCF(2,6).

Mechanochemistry has undergone considerable development over the last two decades. This has included investigations of how polymer chains break and how otherwise inaccessible reaction pathways can be exploited to improve addition polymerisation rates[23] and to provide visible changes to polymers that have been subjected to mechanical stress.[24] Experimental studies have used atomic force microscopy to study the mechanical strength of individual polymer chains,[15,21] ultrasound to open up reaction pathways in mechanophores contained in dissolved polymers[22,23] and externally applied force to macroscale polymer samples.[24] In parallel, theoretical mechanochemistry has developed to relate to the experimental work. The constrained-geometry-to-generate-external-force (COGEF) method[16] uses relaxed potential energy scans to determine atomic forces. In this method a constraint variable is scanned stepwise with the atomic positions allowed to relax at each step. The peak forces found in these scans can then be used to construct Morse potentials for use in calculations of the kinetics of bond rupture. An alternative method, external-force-is-explicitly-included (EFEI),[25] applies forces to the atoms during the optimisation process. Although this allows the determination of the structural response to the applied force mapping of the post-peak-force landscape is difficult. Both methods can be used to determine which bond breaks in a particular molecule but it is equally important to understand why a specific bond breaks. Both the peak restorative force of a bond and the alignment of the bond relative to an applied force determine whether it will or will not fail.[26] Analysis of the Hessian matrix of a molecule, using a redundant internal coordinate system, provides one way for calculating the distribution of energy within the conformal degrees of freedom for a molecular structure. This method, called the judgement of energy distribution (JEDI),[27] can be used to study how

stress is distributed throughout a molecule. A combination of these methods can be used to find transition states for mechanochemically induced reactions but an alternative method for mapping such reaction pathways has also been developed.[28] This method notes that as an increasing external force is applied to a molecule the potential energy surface changes shape causing transition and reactant states move towards each other until they collide at which point the system is no longer well defined. By making a cubic approximation for the potential energy as a function of the reaction coordinate at this point the method allows for the determination of the entire mechanochemical pathway through the reaction space to be determined. In the work presented here there is only a single reactant state minimum which disappears from the potential energy surface as the external applied force is increased. For this reason a relaxed scanning method, similar to the COGEF method is employed here.

In this work, calculations on small hydrocarbon molecules are carried out, over wide ranges of carbon-carbon bond lengths, in order to determine the peak restorative forces and the bond lengths at which they occur. A range of techniques from computationally expensive multi-reference calculations down to much cheaper molecular-mechanics methods are examined and compared. We examine whether multi-reference methods are required to calculate accurate peak restorative forces and corresponding bond lengths. Finally, we investigate the effect of the environment of the bond on its peak restorative force.

Methods

Theoretical methods

In this paper we study bond breaking in ethene, ethane, butane, trans-β-butene (henceforth referred to as butene), isobutane and isobutene (see figure 2). These molecules were selected as they include both single and double carbon bonds and allow examination of the effect of the local environment on individual bond breaking. Single carbon-carbon bonds connecting atoms indicated by the superscripts A and B in figure 2 were extended to just beyond the

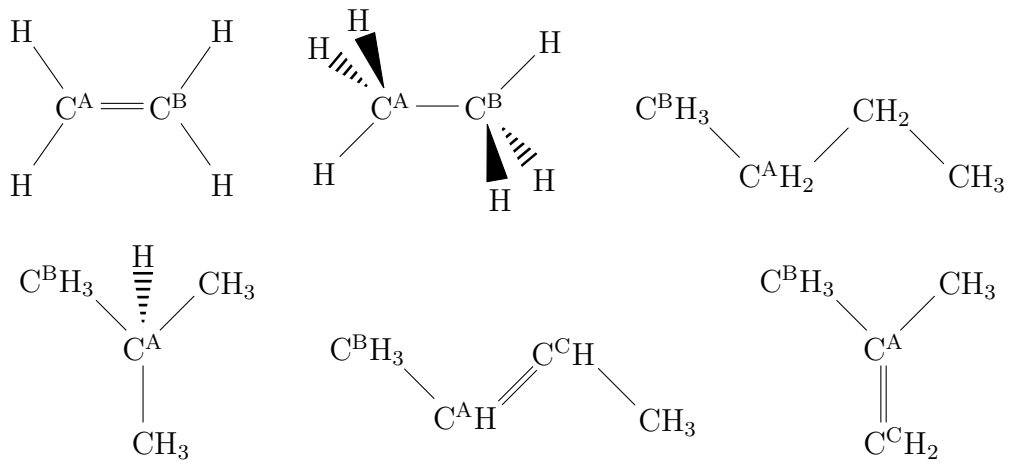

Figure 2: The structures of ethene, ethane, butane, isobutane, trans-β-butene and isobutene. The superscripts A,B and C indicate carbon atoms that were manipulated in the bond length scans.

point of peak restorative force. Double bonds connecting atoms marked by the superscripts A and C were tested independently from the single bond tests.

Potential energy curves were generated for a range of small hydrocarbon molecules. The internuclear distance for a bonded pair of carbon atoms was increased in steps of 0.01 Å. At each step the molecular geometry was optimised, allowing all other atoms to relax. This well known method is conceptually similar to the COGEF method but it scans a well defined molecular internal coordinate rather than a redundant coordinate involving pairs of atoms separated by large distances and multiple bonds. The total energy and force along the bond direction were calculated and plotted as a function of internuclear distance. The peak restorative force is defined as the maximum value of $\mathrm{d}E/\mathrm{d}R$ at bond lengths greater than the equilibrium bond length. The magnitude of the peak restorative force is equal to the maximum constant force that can be applied to the atom before molecular fragmentation and dissociation. Restorative forces may still be present at bond lengths greater than that at which the peak occurs but these would be overcome by any external force of magnitude larger than the peak value. We compare the values of the peak restorative force and the corresponding internuclear distance calculated using different computational methods.

A variety of single reference *ab initio* electronic structure techniques, a multi-reference method, density functional tight binding and two popular reactive molecular mechanics potentials were employed for the calculations. The single reference methods include density functional theory (DFT) using a range of exchange-correlation functionals. The PBE[29] functional was used since it is a very popular functional in current use. B3LYP[30,31] was also selected as it is the most commonly used hybrid functional in DFT calculations. Finally, the more recent B2PLYPD3[32] was chosen as it contains both exact exchange, a perturbation theory based correlation correction and a dispersion term. The other single reference method tested was Møller-Plesset perturbation theory,[33] MP2, which is capable of recovering significant amounts of dynamic correlation.

Complete-active-space-self-consistent-field (CASSCF) calculations were performed to investigate the relevance of the multi-reference nature of bond breaking events. At the point of scission, the electronic wavefunction is best described by sums of multiple degenerate or nearly degenerate determinants. Multi-configuration methods, such as CASSCF, capture these static correlation effects, unlike single-reference methods, which use only a single determinant. The orbitals that were included in the active space were chosen by running a single point calculation and then generating and visualising the natural bond orbitals. In general, the bonding and anti-bonding orbitals related to all the carbon-carbon bonds and the carbon-hydrogen bonds adjacent to the stretched bond were included. This led to an active space of (12,12) for ethene, butene, isobutene and isobutane and an active space of (14,14) for ethane and butane. Due to the computational cost of this method only a handful of geometry steps were investigated for all the molecules except for ethene and ethane where the active space included all valence electrons. For the larger molecules MP2 geometries close to the point of scission were obtained and then reoptimised using the CASSCF method with the length of the bond under investigation fixed appropriately. The natural bond orbitals were inspected to ensure the same active space was used for each optimisation.

These unrestricted spin calculations were performed using Gaussian 09.[34] The PVTZ

basis set (cc-PTVZ)[35] was selected as it offered the best balance between accuracy and computational speed. Higher zeta and augmented basis sets were tested using ethane and ethene and the maximum forces were the same to two significant figures as those from the cc-PTVZ calculations.

These methods are all computationally expensive calculations and are unfeasible for systems containing thousands of atoms. Nevertheless, they do provide useful benchmarks against which computationally cheaper methods can be tested. Two commonly used methods for larger systems and simulating nanostructure failure are the reactive molecular mechanics potentials REBO and ReaxFF. Brenner's reactive empirical bond order potential (REBO)[7] and its derivatives have been widely used for modelling hydrocarbon nanostructures.[10,36,37] Different parametrisations of this potential have also been used for boron nitride based structures.[38,39] This potential and its derivatives have been implemented in many popular atomistic modelling packages. Here, the adaptive intermolecular REBO (AIREBO)[40] variant as implemented in LAMMPS[41] was used. The AIREBO potential was modified to reduce the range of the switching function which reduces carbon-carbon interactions to zero, as suggested in earlier work;[42] the switching function is converted from a cosine form to a step function at 2.0 Å.

The other reactive potential considered here is ReaxFF.[8] This is also available in LAMMPS with a number of different parametrisations so the default parameter files that are distributed with the software were employed.

Finally, density-functional tight-binding (DFTB) was used as implemented in DFTB+.[43] This is described as a non-orthogonal electronic structure method as it does not guarantee exactly orthogonal electron orbitals unlike those generated using self-consistent field methods. This method has three main variants: non-self-consistent-charge (non-SCC-DFTB),[44,45] self-consistent-charge (SCC-DFTB)[46] and third-order self-consistent-charge (DFTB3).[47] The non-SCC variant does not take account of charge transfer between the atoms whereas SCC-DFTB includes charge transfer by way of a second order approximation of DFT. DFTB3

includes third-order corrections by allowing atomic hardness to vary as a function of the charge on each atom. DFTB relies on parameter sets based on DFT calculations using artificially constrained electron densities to provide two-centre Fock and overlap matrix elements over a range of internuclear distances. Once these matrix entries are determined, a repulsive potential is fitted by calculating the difference in energy between DFTB and high quality *ab initio* calculations for various test molecules. Charge self-consistency is determined by including an internuclear partial charge term using atomic hardness parameters. Third order DFTB extends the SCC correction using the gradient of the atomic hardness. The method has also been extended to include unrestricted spin calculations which requires additional parameters. There are three main parameter sets available for DFTB, each reflecting a different stage of the development of the method. The oldest set used here is referred to here as pbc, the next mio and the most recent set 3ob. The pbc and mio sets are both usable for SCC calculations but the 3ob set is described by its authors as only suitable for DFTB3 based calculations.[48] These all contain parameters for hydrogen and carbon.

Results and discussion

Single bonds

The predicted peak restorative forces for the carbon-carbon single bonds studied are presented in table 1 and the corresponding bond lengths listed in table 2. The DFT and MP2 calculations produce fairly consistent predictions for the failure bond length ≈ 1.95 Å but the difference in peak force between the PBE and MP2 results is about 12%. Both MP2 and B2PLYPD3 methods incorporate similar terms for the correlation energy and the restorative forces from both were greater than those from PBE and B3LYP. The CASSCF calculations were performed using fourteen electrons and fourteen orbitals such that all valence electrons and bonding and corresponding antibonding orbitals were included. The CASSCF result

Table 1: Peak restorative forces for carbon-carbon single bond simulations (nN).

Method	Ethane	Butane	Isobutane	Butene	Isobutene
AIREBO	4.90	4.89	4.88	5.24	5.36
ReaxFF	11.05	16.03	18.56	11.71	15.46
DFTB3	6.70	6.35	5.94	6.85	6.56
PBE	5.89	5.71	5.50	6.38	6.08
B3LYP	6.05	5.90	5.70	6.57	6.30
B2PLYPD3	6.20	6.04	5.87	6.74	6.51
MP2	6.59	6.43	6.30	7.09	6.86
CASSCF	5.83	5.56	5.45	6.08	6.10

Table 2: Bond lengths at peak force for carbon-carbon single bond simulations (Å).

Method	Ethane	Butane	Isobutane	Butene	Isobutene
AIREBO	1.88	1.88	1.89	1.85	1.85
ReaxFF	1.98	2.08	2.04	1.79	1.89
DFTB3	1.96	1.96	1.96	1.93	1.94
PBE	1.97	1.96	1.96	1.94	1.94
B3LYP	1.98	1.97	1.97	1.95	1.95
B2PLYPD3	1.96	1.94	1.94	1.93	1.93
MP2	1.98	1.97	1.97	1.94	1.94
CASSCF	1.98	1.97	1.97	1.95	1.96

is remarkably similar to that calculated using the PBE functional, both of which suggest a significantly lower peak force than MP2. This suggests that the dynamic correlation recovered by MP2 is less important for the peak force value than the static correlation recovered by CASSCF.

The self-consistent field electronic structure methods all show the same trends in the variation of the peak force with the number of carbon atoms bonded to the two atoms involved in the bond extension. For molecules involving single carbon-carbon bonds, the bond between the two primary carbon atoms in ethane generates the largest restorative force, followed by the primary-secondary bond in butane and then the primary-tertiary bond in isobutane. A similar pattern is seen with butene and isobutene but the presence of the double bond in these molecules increases the maximum restorative force compared to butane and isobutane.

The variation in peak forces was also compared with that in bond dissociation energies (BDEs) calculated at the MP2/CC-PVTZ level of theory. The BDEs mostly followed the same trends as the peak forces except for ethane which has a marginally lower BDE than butane (≈ 0.004 eV). These variations are displayed graphically in figure 3.

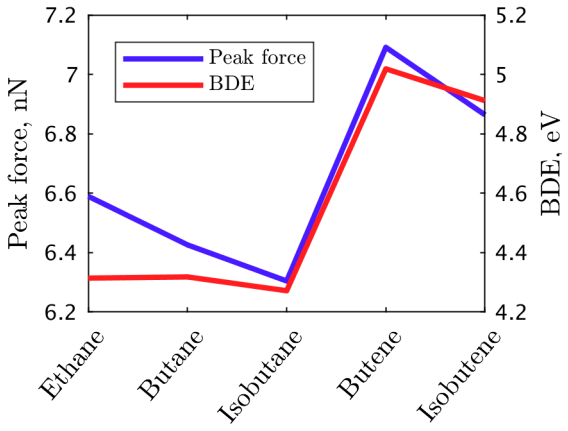

Figure 3: The peak force and the BDE for the single bond dissociations as calculated using MP2/CC-PVTZ.

The AIREBO result provides a smooth variation in the restorative force with internuclear

separation up to the discontinuity in the energy at 2.0 Å caused by the step-wise cut-off function as shown in figure 4. The AIREBO data indicate a weaker restorative force than

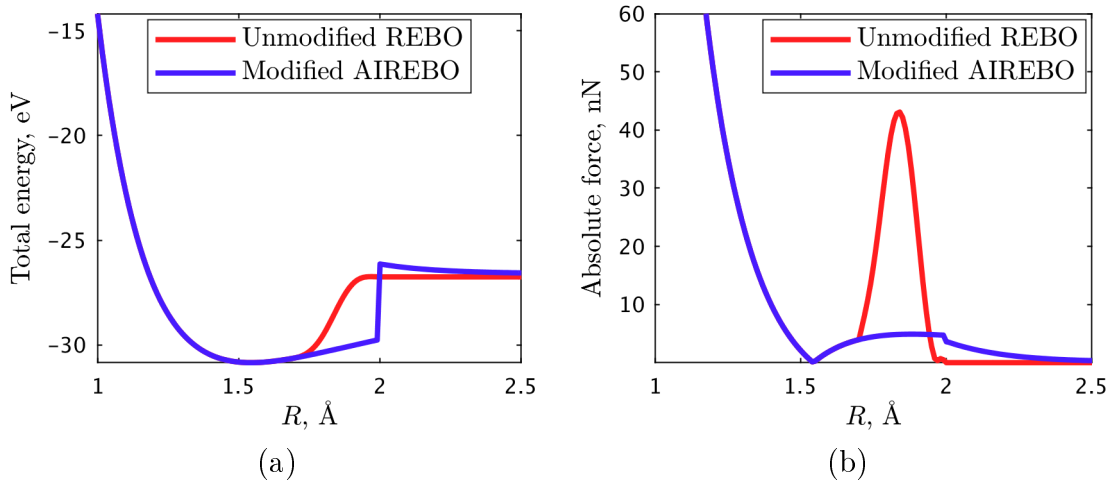

Figure 4: Energy (a) and force (b) plotted as functions of internuclear separation for the carbon-carbon bond in ethane calculated using both the original and modified REBO potentials. The overbinding caused by the energy cutoff function can be seen in the REBO result and the discontinuous energy can be seen in the AIREBO result.

the electronic structure methods but the peak force appears to vary with the environment of the stretched bond in a similar manner to the higher-order methods. The peak forces for the single bonds in butene and isobutene as calculated by AIREBO are greater than that for the other molecules, which agrees with the electronic structure results but this effect is less pronounced.

ReaxFF generates very poor forces in comparison to the *ab initio* methods and indeed struggles to produce reasonable energy curves as can be seen in figure 5. The cause of the erroneous peak at approximately 1.25 Å for ethane is the bond order calculation used in ReaxFF. This potential uses a function which is the sum of three exponential functions of interatomic distance to determine a bond order that varies continuously from zero to three for a carbon-carbon bond. One of the exponential terms tends to zero at the bond length corresponding to the erroneous force peak. After the minimum energy at 1.59 Å in figure 5, the magnitude of the force rises steadily before reaching a plateau followed by a peak at 2.0 Å. This non-physical behaviour appears due to the bond order function as first one of

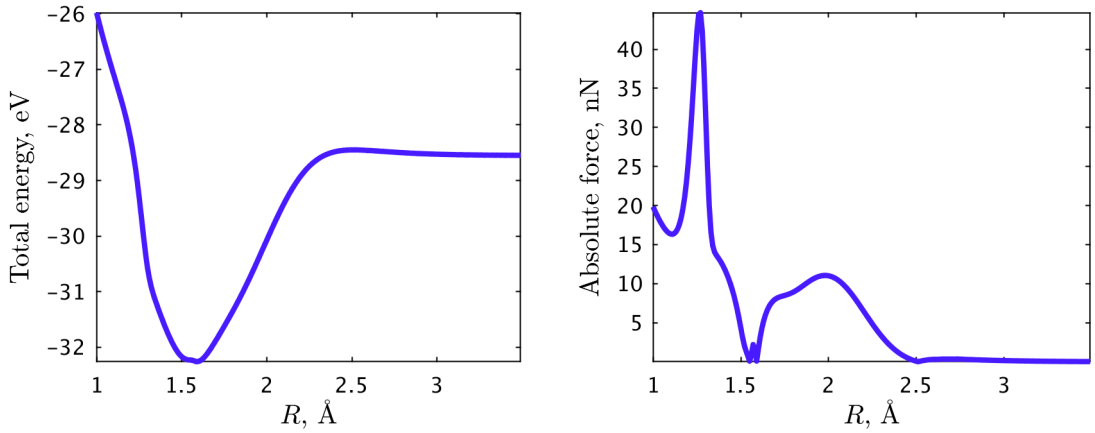

Figure 5: Energy and force plotted as functions of internuclear separation for the carbon-carbon bond in ethane calculated using ReaxFF. The poor approximation of the energy curve results in an even worse approximation of the forces.

the exponential terms and then another tends to zero. The curvature of these terms is lower and so the corresponding peaks in the force are less pronounced.

Only results for DFTB3 are given due to erroneous forces present in the SCC-DFTB calculations which can be seen in figure 6. The earlier parameter sets used in non-DFTB3

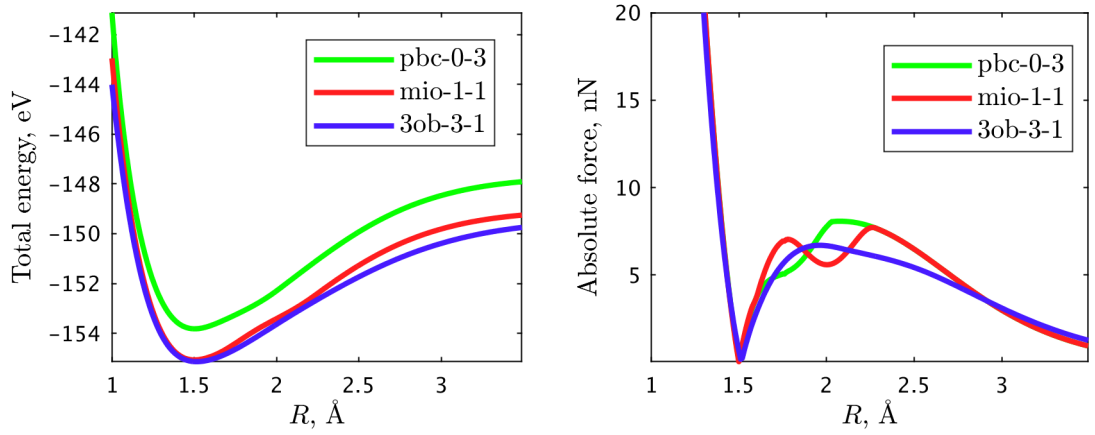

Figure 6: Energy and force plotted as functions of internuclear separation for the carbon-carbon bond in ethane calculated using different DFTB variants. The poor approximation of the energy curve results in an even worse approximation of the forces.

calculations produce unphysical force displacement plots with a characteristic double peak.

The cause is the repulsive potential, a sum of pairwise interaction terms which includes ionic repulsion and exchange-correlation contributions among others, used within the DFTB parameter sets. This potential can be considered the DFTB analogue for the exchange-correlation functional of DFT.[49] It is calculated as the difference between the sum of the tight-binding band structure and Coulomb energies and a total energy calculated from higher accuracy calculations. This potential is then represented by an exponential function at short range, then a series of cubic splines at intermediate distances and finally a fifth order spline. The role of the fifth order spline is to provide continuous first and second derivatives with the preceding cubic spline and to force the potential and its derivatives to zero at some cutoff distance. The fifth order splines used in earlier DFTB parameter sets cause erroneous, albeit continuous, force curves.

Encouragingly, in contrast to the earlier DFTB parameters, DFTB3 results are physically reasonable. They show slightly higher restorative forces than the higher order electronic structure methods but the location of the peaks are in good agreement. The environment of the bond appears to influence the restorative forces calculated using DFTB3 in the same way as the higher order electronic structure calculations. All the results show the same environment-dependent variation of the failure bond length for single bonds.

Double bonds

The predicted peak restorative forces for carbon-carbon double bonds are presented in table 3 and the corresponding bond lengths at which they occur are in table 4. DFT and MP2 calculations predict fairly consistent bond failure lengths of ≈ 1.73 Å for the double bonds. PBE and B3LYP results indicate a longer failure bond length for the double bond simulations than MP2 and B2PLYPD3. The peak forces of B3LYP are consistently greater than the other DFT functionals and MP2 calculations. The CASSCF calculations show lower peak forces than all the other electronic structure methods investigated here. The results show that single reference methods may overestimate peak restorative forces but the

Table 3: Peak restorative forces for carbon-carbon double bonds (nN).

Method	Ethene	Butene	Isobutene
AIREBO	9.52	9.66	9.72
ReaxFF	30.07	24.33	25.04
DFTB3	13.90	12.98	12.92
PBE	13.04	12.35	12.23
B3LYP	13.80	13.19	13.10
B2PLYPD3	13.17	12.69	12.68
MP2	12.83	12.29	12.64
CASSCF	12.03	12.10	12.17

Table 4: Bond lengths at peak-force for carbon-carbon double bonds (Å).

Method	Ethene	Butene	Isobutene
AIREBO	1.60	1.59	1.59
ReaxFF	1.59	1.60	1.60
DFTB3	1.71	1.72	1.73
PBE	1.75	1.74	1.75
B3LYP	1.75	1.74	1.74
B2PLYPD3	1.72	1.72	1.73
MP2	1.71	1.71	1.75
CASSCF	1.73	1.74	1.75

corresponding bond lengths will be within a few percent of those calculated using multi reference methods.

The BDEs follow a similar trend to the peak force calculations, as shown in figure 7. The

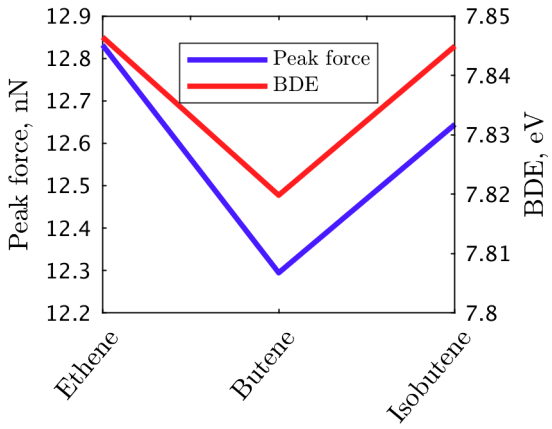

Figure 7: The peak force and the BDE for the double bond dissociations calculated using MP2/CC-PVTZ.

peak forces and BDEs are both larger than the those for single bonds.

The AIREBO results underestimate the bond strength and failure bond lengths for double bonds, as it did for the single bonds. ReaxFF massively overestimates the restorative forces and fails to reproduce the failure bond lengths seen in DFT or MP2.

The results from this work highlight the difficulty of trying to find reliable estimates for peak restorative forces. There is considerable variation of this property even when only the electronic structure calculations are considered. The average standard deviation of the peak force across the different molecules is 5.4 % for single bonds and 3.8 % for double bonds. Differences of up to 1 or 2 nN can be seen between different *ab initio* methods for certain molecules. This makes it difficult to draw any conclusions about which method is the most reliable for predicting these properties, even though qualitative trends are consistent.

The multireference CASSCF values are lower for all cases except for the single bond in isobutene where PBE produced a marginally smaller value. The dynamic correlation energy, as calculated using MP2 and B2PLYPD3, increases the peak force values for the single bonds

but lowers them for the double bonds. These lower values are close to those calculated using CASSCF which suggests the multireference nature of bond breaking events are less important when considering double bonds. This is evident in the difference between the occupancy of the CASSCF orbitals in the tests of double and single bonds. Obviously, for single bonds only the σ-orbital at the point of peak restorative force is active in the CASSCF active space. As this orbital is solely responsible for the restorative force the multireference effects influence the calculated values. For double bonds, the occupancy of the π-orbital is reduced while that of the σ-orbital is not. Here, the multireference nature of bond breaking is less relevant as both the π- and σ-orbitals are responsible for generating the restorative force but only the π-orbital is active in the CASSCF space.

The results presented here show the effect of the local environment of a bond on its peak restorative force is two-fold. First, the peak restorative force for a bond involving only primary carbon atoms is larger than that between a primary and a secondary carbon atom, which in turn is larger than that between a primary and a tertiary carbon atom. Second, the presence of a double bond adjacent to a single bond increases the single bonds peak restorative force, as shown in a comparison of the results for single bonds using butane/butene and isobutane/isobutene.

The electronic structure results, although they vary in magnitude, do provide some benchmark for comparison with the molecular mechanics potentials. Of the two potentials investigated, the AIREBO potential is clearly the superior. ReaxFF produced inconsistent results; testing of similar carbon-carbon bonds in different molecules produced a significant spread in both peak restorative forces and the corresponding bond lengths. ReaxFF peak forces were much higher than those of any other method and did not follow the general trends seen in the results from electronic structure methods. AIREBO did at least reproduce the trends seen with the electronic structure methods regarding whether the molecule contained a carbon-carbon double bond and between primary, secondary and tertiary carbons. However, it consistently predicted lower peak restorative forces and shorter corresponding bond lengths.

This potential may provide qualitatively correct behaviour when simulating catastrophic failure of carbon structures but it will most likely underestimate the forces required to cause failure and the structures strain at failure. The hard cutoff required to use this potential for these types of simulations may also cause other problems when attempting such simulations.

Conclusions

This work has compared different methods for calculating forces between carbon atoms for a range of bond lengths. Peak restorative forces, an analogue for mechanical strength, and the bond lengths at which they occur have been calculated for a range of carbon-carbon bonds occurring in a variety of different molecules. The type and environment of the bond was shown to influence the peak restorative force and the bond failure length. These data provide a useful benchmark for testing other methods for calculating such forces.

Single bonds between two carbon atoms, where one of these atoms is doubly bonded to a third atom, show greater maximum restorative forces and slightly shorter bond failure lengths compared to carbon atoms involved in only single bonds. The peak restorative forces of single bonds involving a primary carbon atom decrease as the other atom in the bond changes form primary to secondary to tertiary. Carbon-carbon double bonds have larger peak restorative forces at smaller bond lengths than single bonds. The qualitative variation of bond dissociation energies from molecule to molecule is similar to that of peak force, but the correlation is not sufficiently strong to allow accurate prediction of the force solely from knowledge of the BDE.

The unmodified REBO and the ReaxFF force displacement curves show significant errors and cannot be relied upon for simulations of nanostructures under stretch to failure type conditions. The modified AIREBO results show lower peak restorative forces and shorter failure bond lengths compared to the electronic structure methods for all bond types considered. Although the modified potential may not provide accurate quantitative results, the qualitative

behaviour seen in this work was superior to ReaxFF. However, the inclusion of the switching function produces erroneous forces near the peak restorative force but its removal creates discontinuous energies and forces. Applying such a cutoff produces unreliable behaviour in any situation where a bond breaks but the atoms involved in the bond are still relatively close together. Overall the results show DFTB3 and the higher order electronic structure methods are in reasonable agreement, producing qualitatively similar variations of the measured properties with bond type and environment.

Prediction of the forces between atomic nuclei is extremely difficult. Molecular mechanics potentials, which are computationally cheap even for relatively large nanostructures, can suffer from non-physical behaviour either due to discontinuous energies and gradients or due to poor choice of switching functions. Even complex and computationally expensive electronic structure calculations struggle to agree over large ranges of internuclear separation. Parametrised methods such as DFTB3 can produce reasonable results in comparison to higher order methods but only if the parametrisation is performed with care. This is particularly encouraging for future applications to much larger structures.

Acknowledgement

This work was supported by the Engineering and Physical Sciences Research Council through the EPSRC Centre for Doctoral Training in Advanced Composites for Innovation and Science [grant number EP/L016028/1].

Supporting Information Available

References

(1) Baran, J. D.; Eames, C.; Takahashi, K.; Molinari, M.; Islam, M. S.; Parker, S. C. Structural, Electronic, and Transport Properties of Hybrid SrTiO3-Graphene and

Carbon Nanoribbon Interfaces. *Chemistry of Materials* **2017**, *29*, 7364–7370.

(2) Hart, J. N.; Parker, S. C.; Lapkin, A. A. Energy Minimization of Single-Walled Titanium Oxide Nanotubes. *ACS Nano* **2009**, *3*, 3401–3412.

(3) Cohen-Tanugi, D.; Grossman, J. C. Water Desalination across Nanoporous Graphene. *Nano Letters* **2012**, *12*, 3602–3608.

(4) Kim, H.; Lee, K.; Woo, S. I.; Jung, Y. On the mechanism of enhanced oxygen reduction reaction in nitrogen-doped graphene nanoribbons. *Physical Chemistry Chemical Physics* **2011**, *13*, 17505.

(5) Rafiee, M. A.; Lu, W.; Thomas, A. V.; Zandiatashbar, A.; Rafiee, J.; Tour, J. M.; Koratkar, N. a. Graphene Nanoribbon Composites. *ACS Nano* **2010**, *4*, 7415–7420.

(6) Tersoff, J. New empirical approach for the structure and energy of covalent systems. *Physical Review B* **1988**, *37*, 6991–7000.

(7) Brenner, D. W. Empirical potential for hydrocarbons for use in simulating the chemical vapor deposition of diamond films. *Physical Review B* **1990**, *42*, 9458–9471.

(8) van Duin, A. C. T.; Dasgupta, S.; Lorant, F.; Goddard, W. A. ReaxFF: A Reactive Force Field for Hydrocarbons. *Journal of Physical Chemistry A* **2001**, *105*, 9396–9409.

(9) Zhao, H.; Min, K.; Aluru, N. R. Size and Chirality Dependent Elastic Properties of Graphene Nanoribbons under Uniaxial Tension. *Nano Letters* **2009**, *9*, 3012–3015.

(10) Lu, Q.; Gao, W.; Huang, R. Atomistic simulation and continuum modeling of graphene nanoribbons under uniaxial tension. *Modelling and Simulation in Materials Science and Engineering* **2011**, *19*, 054006.

(11) Bizao, R.; Botari, T.; Perim, E.; Pugno, N.; Galvao, D. Mechanical properties and fracture patterns of graphene (graphitic) nanowiggles. *Carbon* **2017**, *119*, 431–437.

(12) Zhao, H.; Aluru, N. R. Temperature and strain-rate dependent fracture strength of graphene. *Journal of Applied Physics* **2010**, *108*, 064321.

(13) Kim, K.; Artyukhov, V. I.; Regan, W.; Liu, Y.; Crommie, M. F.; Yakobson, B. I.; Zettl, A. Ripping Graphene: Preferred Directions. *Nano Letters* **2012**, *12*, 293–297.

(14) Zhang, T.; Li, X.; Kadkhodaei, S.; Gao, H. Flaw Insensitive Fracture in Nanocrystalline Graphene. *Nano Letters* **2012**, *12*, 4605–4610.

(15) Grandbois, M.; Beyer, M.; Rief, M.; Clausen-Schaumann, H.; Gaub, H. E. How Strong Is a Covalent Bond? *Science* **1999**, *283*, 1727–1730.

(16) Beyer, M. K. The mechanical strength of a covalent bond calculated by density functional theory. *Journal of Chemical Physics* **2000**, *112*, 7307–7312.

(17) Dutta, A.; Sherrill, C. D. Full configuration interaction potential energy curves for breaking bonds to hydrogen: An assessment of single-reference correlation methods. *Journal of Chemical Physics* **2003**, *118*, 1610–1619.

(18) Iozzi, M. F.; Helgaker, T.; Uggerud, E. Assessment of theoretical methods for the determination of the mechanochemical strength of covalent bonds. *Molecular Physics* **2009**, *107*, 2537–2546.

(19) Kochhar, G. S.; Bailey, A.; Mosey, N. J. Competition between Orbitals and Stress in Mechanochemistry. *Angewandte Chemie International Edition* **2010**, *49*, 7452–7455.

(20) Kedziora, G. S.; Barr, S. A.; Berry, R.; Moller, J. C.; Breitzman, T. D. Bond breaking in stretched molecules: multi-reference methods versus density functional theory. *Theoretical Chemistry Accounts* **2016**, *135*, 79.

(21) Zou, S.; Schönherr, H.; Vancso, G. J. Stretching and rupturing individual supramolecular polymer-chains by AFM. *Angewandte Chemie - International Edition* **2005**, *44*, 956–959.

(22) Hickenboth, C. R.; Moore, J. S.; White, S. R.; Sottos, N. R.; Baudry, J.; Wilson, S. R. Biasing reaction pathways with mechanical force. *Nature* **2007**, *446*, 423–427.

(23) Potisek, S. L.; Davis, D. A.; Sottos, N. R.; White, S. R.; Moore, J. S. Mechanophore-Linked Addition Polymers. *Journal of the American Chemical Society* **2007**, *129*, 13808–13809.

(24) Davis, D. A.; Hamilton, A.; Yang, J.; Cremar, L. D.; Van Gough, D.; Potisek, S. L.; Ong, M. T.; Braun, P. V.; Martínez, T. J.; White, S. R.; Moore, J. S.; Sottos, N. R. Force-induced activation of covalent bonds in mechanoresponsive polymeric materials. *Nature* **2009**, *459*, 68–72.

(25) Ribas-Arino, J.; Shiga, M.; Marx, D. Understanding Covalent Mechanochemistry. *Angewandte Chemie International Edition* **2009**, *48*, 4190–4193.

(26) Smalø, H. S.; Uggerud, E. Breaking covalent bonds using mechanical force, which bond breaks? *Molecular Physics* **2013**, *111*, 1563–1573.

(27) Stauch, T.; Dreuw, A. A quantitative quantum-chemical analysis tool for the distribution of mechanical force in molecules. *Journal of Chemical Physics* **2014**, *140*, 134107.

(28) Avdoshenko, S. M.; Makarov, D. E. Finding mechanochemical pathways and barriers without transition state search. *Journal of Chemical Physics* **2015**, *142*, 174106.

(29) Perdew, J. P.; Burke, K.; Ernzerhof, M. Generalized Gradient Approximation Made Simple. *Physical Review Letters* **1996**, *77*, 3865–3868.

(30) Lee, C.; Yang, W.; Parr, R. G. Development of the Colle-Salvetti correlation-energy formula into a functional of the electron density. *Physical Review B* **1988**, *37*, 785–789.

(31) Becke, A. D. Density-functional thermochemistry. III. The role of exact exchange. *Journal of Chemical Physics* **1993**, *98*, 5648–5652.

(32) Grimme, S. Semiempirical hybrid density functional with perturbative second-order correlation. *Journal of Chemical Physics* **2006**, *124*, 034108.

(33) Møller, C.; Plesset, M. S. Note on an Approximation Treatment for Many-Electron Systems. *Physical Review* **1934**, *46*, 618–622.

(34) Frisch, M. J. et al. Gaussian 09, Revision D.01. 2013; Gaussian Inc. Wallingford CT.

(35) Dunning, T. H. Gaussian basis sets for use in correlated molecular calculations. I. The atoms boron through neon and hydrogen. *Journal of Chemical Physics* **1989**, *90*, 1007–1023.

(36) Cornwell, C.; Wille, L. Elastic properties of single-walled carbon nanotubes in compression. *Solid State Communications* **1997**, *101*, 555–558.

(37) Liu, Y.; Chen, X. Mechanical properties of nanoporous graphene membrane. *Journal of Applied Physics* **2014**, *115*, 034303.

(38) Verma, V.; Jindal, V. K.; Dharamvir, K. Elastic moduli of a boron nitride nanotube. *Nanotechnology* **2007**, *18*, 435711.

(39) Anoop Krishnan, N. M.; Ghosh, D. Chirality dependent elastic properties of single-walled boron nitride nanotubes under uniaxial and torsional loading. *Journal of Applied Physics* **2014**, *115*, 064303.

(40) Stuart, S. J.; Tutein, A. B.; Harrison, J. A. A reactive potential for hydrocarbons with intermolecular interactions. *Journal of Chemical Physics* **2000**, *112*, 6472–6486.

(41) Plimpton, S. Fast Parallel Algorithms for Short-Range Molecular Dynamics. *Journal of Computational Physics* **1995**, *117*, 1–19.

(42) Shenderova, O. a.; Brenner, D. W.; Omeltchenko, A.; Su, X.; Yang, L. H. Atomistic modeling of the fracture of polycrystalline diamond. *Physical Review B* **2000**, *61*, 3877–3888.

(43) Aradi, B.; Hourahine, B.; Frauenheim, T. DFTB+, a sparse matrix-based implementation of the DFTB method. *Journal of Physical Chemistry A* **2007**, *111*, 5678–5684.

(44) Porezag, D.; Frauenheim, T.; Köhler, T.; Seifert, G.; Kaschner, R. Construction of tight-binding-like potentials on the basis of density-functional theory: Application to carbon. *Physical Review B* **1995**, *51*, 12947–12957.

(45) Seifert, G.; Porezag, D.; Frauenheim, T. Calculations of molecules, clusters, and solids with a simplified LCAO-DFT-LDA scheme. *International Journal of Quantum Chemistry* **1996**, *58*, 185–192.

(46) Elstner, M.; Porezag, D.; Jungnickel, G.; Elsner, J.; Haugk, M.; Frauenheim, T.; Suhai, S.; Seifert, G. Self-consistent-charge density-functional tight-binding method for simulations of complex materials properties. *Physical Review B* **1998**, *58*, 7260–7268.

(47) Yang, Y.; Yu, H.; York, D.; Cui, Q.; Elstner, M. Extension of the self-consistent-charge density-functional tight-binding method: Third-order expansion of the density functional theory total energy and introduction of a modified effective coulomb interaction. *Journal of Physical Chemistry A* **2007**, *111*, 10861–10873.

(48) Gaus, M.; Goez, A.; Elstner, M. Parametrization and Benchmark of DFTB3 for Organic Molecules. *Journal of Chemical Theory and Computation* **2013**, *9*, 338–354.

(49) Koskinen, P.; Mäkinen, V. Density-functional tight-binding for beginners. *Computational Materials Science* **2009**, *47*, 237–253.

Graphical TOC Entry